Hierarchical Cluster Coordination Control Strategy for Large-scale Wind Power Based on Model Predictive Control and Improved Multi-time-scale Active Power Dispatching

Ying Zhu, Yanan Zhang, and Zhinong Wei

***Abstract*—The grid-connection of large-scale and high-penetration wind power poses challenges to the friendly dispatching control of the power system. To coordinate the complicated optimal dispatching and rapid real-time control, this paper proposes a hierarchical cluster coordination control (HCCC) strategy based on model predictive control (MPC) technique. Considering the time-varying characteristics of wind power generation, the proposed HCCC strategy constructs an improved multi-time-scale active power dispatching model, which consists of five parts: formulation of cluster dispatching plan, rolling modification of intra-cluster plan, optimization allocation of wind farm (WF), grouping coordinated control of wind turbine group (WTG), and real-time adjustment of single-machine power. The time resolutions are sequentially given as 1 hour, 30 min, 15 min, 5 min, and 1 min. In addition, a combined predictive model based on complete ensemble empirical mode decomposition with adaptive noise (CEEMDAN), wavelet thresholding (WT), and least squares support vector machine (LSSVM) is established. The fast predictive feature of this model cooperates with the HCCC strategy that effectively improves the predictive control precision. Simulation results show that the proposed HCCC strategy enables rapid response to active power control (APC), and significantly improves dispatching control accuracy and wind power accommodation capabilities.**

***Index Terms*—Wind power, active power dispatching, model predictive control (MPC), hierarchical control, wind power prediction.**

I. Introduction

REACHING carbon emission peak and carbon neutrality are the ultimate goal of modern energy systems [1]. As a clean, environmentally-friendly, and low-cost renewable energy source, wind energy has enormous commercial potential and has been developed and utilized worldwide [2]. Due to the reverse distribution of wind energy resources and load centers, the exploitation and accommodation of wind power in China are mainly based on a large-scale and centralized mode. However, with the clustering of wind power grid-connection and the expansion of single-machine capacity, the grid adaptability problem has become more prominent. The uncertainty and anti-peak shaving characteristics of wind power aggravate the phenomenon of regional wind curtailment [3]-[6]. Thus, some forecasting technologies and dispatching modes have been considered to mitigate the negative effects of wind power integration. Due to the limited improvement in predictive accuracy, transforming traditional dispatching modes and developing new dispatching strategies can be more readily achieved. Consequently, the formulation of active power dispatching (APD) schemes, which can effectively cope with the inherent characteristics of wind power, has become a research hotspot [7]-[11].

The conventional dispatching mode comprises only day-ahead dispatching and automatic generation control (AGC), resulting in a major contradiction between the accuracy of wind power prediction (WPP) and the forward-looking nature of dispatching. Therefore, to overcome the shortcomings of traditional methods such as large errors in tracking dispatching plans and poor active power control (APC) effects, a new idea of mutual coordination of different time scales has been developed in APD considering wind power. Reference [12] proposes an intelligent dispatching model that subdivides APD into four stages: day-ahead planning, intra-day dispatching, real-time control, and AGC. Based on this framework, economic and robust dispatching strategies under multiple temporal scales are proposed for wind power systems in [13] and [14], respectively. The coordinated multi-time-scale optimization strategy refines the operating control instructions step by step and improves the control accuracy and wind power utilization.

In addition, a power system requires flexible and rapid APD control. A comparative analysis of existing dispatching strategies [15]-[18] shows that adding dispatching links with shorter control cycles has a more obvious auxiliary effect on the power system regulation capability. Therefore, intra-day rolling and real-time dispatching play increasingly important

Manuscript received: January 5, 2022; revised: April 29, 2022; accepted: August 3, 2022. Date of CrossCheck: August 3, 2022. Date of online publication: September 14, 2022.

This work was supported in part by the Joint Funds of the National Natural Science Foundation of China (No. U1966205) and Fundamental Research Funds for the Central Universities (No. B210202067).

Y. Zhu (corresponding author), Y. Zhang, and Z. Wei are with the College of Energy and Electrical Engineering, Hohai University, Nanjing 210098, China (e-mail: yingzhu@hhu.edu.cn; zhangynhhu@163.com; znwei@hhu.edu.cn).

DOI: 10.35833/MPCE.2022.000010

roles in multi-time-scale dispatching. In most of the current research, the optimization period of intra-day dispatching is consistent with the maximum predictive time domain of an ultra-short-term WPP, i.e., 4 hours [19]. Although this time scale can revise unreasonable day-ahead generation plans to some extent, the timeliness of the control response can hardly be satisfied. Furthermore, the technological advancements in wind power control can shorten the response time of wind generators (WGs) to active power regulation and increases the unit adjustment speed. To minimize the high-resolution predictive errors and inhibit short-term random fluctuations, refining the dispatching time granularity to reduce dispatching control cycles is essential and feasible.

To deal with the output uncertainty of wind power clusters (WPCs), [20]-[23] introduce the model predictive control (MPC) technique for multi-time-scale optimal APD. As a finite-time-domain rolling optimization control approach, MPC has been applied to APC by many scholars. Reference [21] proposes a distributed economic MPC strategy for APC of wind farms (WFs). This control architecture guarantees dynamic economic optimality while improving power tracking performance. An MPC-based dynamic dispatching strategy for integrated energy systems is introduced in [22]. The trajectory deviation control and output increment control of MPC are used to respond to dispatching demand changes. MPC has also been applied to the coordination control of integrated wind power and energy storage systems [23]. In short, the superiority of MPC is in its ability to adapt to external uncertainties and complex changes through rolling optimization and its ability to increase predictive control precision through feedback correction [24]-[27]. To improve the APD accuracy, this paper applies MPC to the cluster coordination control.

Mathematically, the APC of WPC is essentially a multi-objective optimization problem for a non-linear time-varying system. Given the large discrepancy in the optimization objectives and execution cycles of dispatching and controlling, the decomposition-coordination method [28]-[30] is typically used to alleviate the conflict between complicated dispatching and rapid control in wind power systems. With the goal of improving the dispatchability and controllability of the WPC, [31] and [32] propose a multiple temporal-spatial stratified predictive control method for active power, which ensures the dispatching flexibility and enhances the adaptability of power network. However, the studies on coordinating the optimal distribution of active power between WFs in the WPC remain limited. In addition, a reasonable active power distribution scheme for each WG is recommended, as the bottom control objects of the current hierarchical control are WFs.

To address the aforementioned problems, this paper proposes a hierarchical cluster coordination control (HCCC) strategy based on MPC and decomposition-coordination theory. The main contribution of this paper is the establishment of an improved multi-time-space-scale coordinated operation mechanism for WPCs. Regarding the refinement of time scales, a multi-time-scale coordination model of "1 hour-30 min-15 min-5 min-1 min" is constructed based on the framework of 24-hour day-ahead dispatching, 4-hour intra-day rolling, and 15-min real-time control. For the extension of spatial scales, five control layers are divided according to the control area: WPC, wind farm clusters (WFCs), WFs, wind turbine groups (WTGs), and WGs. In addition, to balance the predictive promptness and accuracy, a least squares support vector machine (LSSVM) predictive model based on complete ensemble empirical mode decomposition with adaptive noise (CEEMDAN) wavelet thresholding (WT) joint denoising is established in this paper. The practicability and validity of the proposed strategy are verified through the analysis of specific numerical examples.

The remainder of this paper is organized as follows. Section II proposes a framework of the HCCC strategy. Section III presents the mathematical modeling of the proposed dispatching scheme based on multiple fine-grained time scales. Section IV provides the detailed formulation of the MPC for WPC active power. Section V analyzes the results of the case testing. Section VI concludes this paper.

II. Framework of HCCC Strategy

The geographical dispersion effect of WFs and the temporal correlation of wind speed causes the overall output of a WPC to present unique spatiotemporal properties. Figure 1 shows the daily power fluctuations of WPC and WFs under various time scales. When the time resolution is less than 1 hour (short time scale), the outputs of WFs are complementary, and thus the power fluctuation of WPC is weakened. Statistics also reveal that the differences exist in the real-time power generation capacities of the three WFs, and the output coordination among them must be addressed. Improper control causes under- or over-regulation on the outputs of WFs. In addition, it can be concluded that wind power fluctuation becomes stronger with a time-scale extension. Accordingly, it is necessary to suppress the disturbances step by step from top to bottom to satisfy the grid-connected criteria. The aforementioned issues represent the motivations for the study of cluster coordination control in this paper.

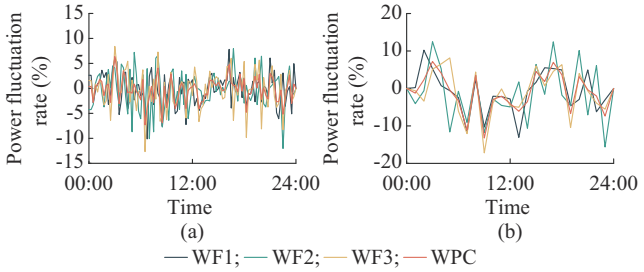

Fig. 1. Power fluctuations of WPC and WFs. (a) Time resolution is 15 min. (b) Time resolution is 1 hour.

Compared with conventional APD schemes, the superiority of the proposed HCCC strategy is mainly manifested in the following two respects.

1) Horizontal coordination at multiple time scales. To balance the dispatching reliability, regulation flexibility, and control rapidity, this paper further refines the control cycles of high-resolution (minute-level) dispatching links. First, we

add a rolling modification link of intra-cluster plan to reduce day-ahead predictive errors and smooth hour-level grid-connected fluctuations. Based on the day-ahead time scale, the optimization period is set to be 1 hour with a rolling interval of 30 min. According to the latest ultra-short-term predictive data, the hourly generation plan is fine-tuned to ensure accurate coordination and optimization between subsequent intra-day and real-time dispatching. In addition, traditional real-time dispatching plays a limited role in amending the latest predictive errors and realizing dynamic power balancing. To make full use of the speedy control response of WGs, the control cycle of real-time dispatching at the WG layer is set to be 1 min in this paper. The refined dispatching time granularity "1 hour-30 min-15 min-5 min-1 min" can progressively absorb WPP errors and weaken the effects of wind power fluctuations.

2) Vertical coordination at multiple spatial scales. The proposed HCCC strategy covers the coordinated optimization among WGs, WTGs, WFs, WFCs, and WPC. Through the decomposition and harmonization within the WPC, a dynamic balance between dispatching optimality and control rapidity is realized. The collaboration among the WPC, WFCs, and WFs improves the dispatchability of the WPC and maximizes the wind accommodation. The coordination and complementation of WTGs and WGs not only realize the scientific distribution of active power but also increase the plan tracking precision and control accuracy.

A framework of the proposed HCCC strategy is presented in Fig. 2. This strategy consists of five parts: ① formulation of cluster dispatching plan; ② rolling modification of intra-cluster plan; ③ optimization allocation of WF; ④ grouping coordinated control of WTG; and ⑤ real-time adjustment of single-machine power.

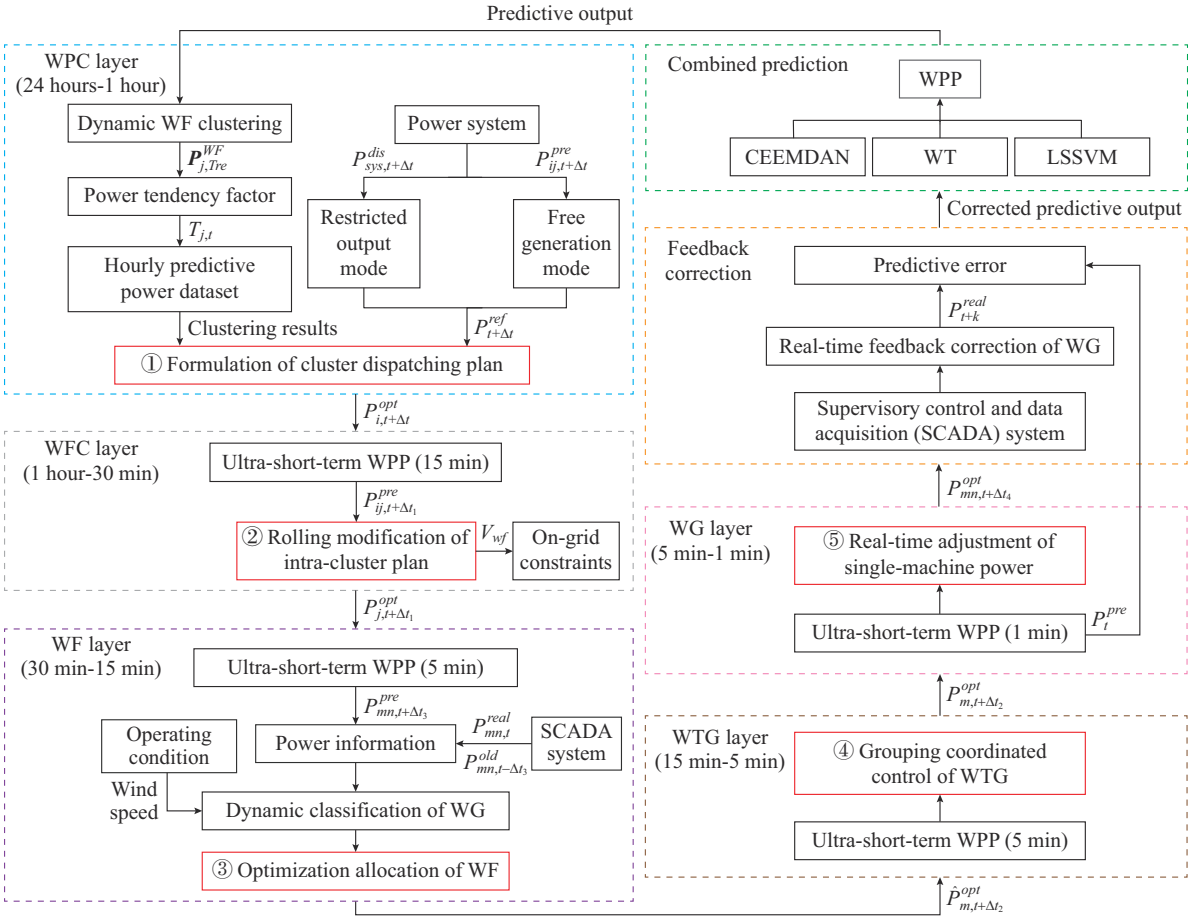

Fig. 2. Framework of HCCC strategy.

1) Formulation of cluster dispatching plan: this link is a type of day-ahead dispatching. In this paper, the WFs are first clustered once per hour according to the trend of the predictive output power. Then, based on the dispatching plan issued by power system and short-term predictive information, the optimal dispatching power of the WPC with the aim of maximizing the output wind power is calculated.

2) Rolling modification of intra-cluster plan: this link is designed to modify unreasonable day-ahead plans to compensate for predictive errors. In addition, to suppress short-term random fluctuations, an allowable fluctuation limit of the power grid within 30 min is introduced to fine-tune the active power commands of each WFC. This improvement ensures dispatching flexibility to accommodate real-time variations.

3) Optimization allocation of WF: WFs play a connecting role in HCCC. Consequently, this link aims to enhance the dispatchability and controllability of the WFs. Within the

control cycle of the rolling modification link for intra-cluster plan, the optimal control is conducted with a rolling period of 15 min to improve the minute-level control accuracy.

4) Grouping coordinated control of WTG: to make the most of the differential regulation performance of units under diverse states, this paper categorizes the units in accordance with their actual operating conditions and power generation potential. Dynamic grouping is beneficial for realizing the scientific allocation of WF active power commands, thereby decreasing the frequency of dispatching fluctuations. The classification cycle coincides with the control cycle of the WF layer. In addition, the optimized power of the wind turbines is then calculated every 5 min based on the grouping results.

5) Real-time adjustment of single-machine power: relying on technological innovation and industry maturity, this paper shortens the real-time dispatching control cycle in the WG from 5 min to 1 min. The purpose is to minimize the control deviation between the active power of the WG and the reference value issued by the WTG layer to approximate actual operating conditions.

III. Mathematical Modeling of HCCC Strategy

A. Formulation of Dynamic WF Clustering Strategy

Constrained by the allowable fluctuation of grid-connected power, this paper aims to maximize the output power of WPC on the premise of safeguarding grid security and reliability. If the output power is improperly coordinated among WFs, there is a risk of wind power penetration overlimit or power shortage. Therefore, to formulate the optimal generation plans for the WPC, this paper first performs dynamic clustering based on the rolling time window for WFs. Considering the control accuracy and operation smoothness, we set the clustering period to be 1 hour. The main principle of dynamic clustering is to evaluate and update the power regulation capacities of WFs based on the trend of predictive power per hour. The clustering index, i. e., the predictive power tendency factor $T_{j,t}$, is calculated by:

$$\boldsymbol{P}_{j,Tre}^{WF}=\left[\bar{P}_{j,t+t_0}^{wf}\quad \bar{P}_{j,t+t_1}^{wf}\quad \bar{P}_{j,t+t_2}^{wf}\quad \bar{P}_{j,t+t_3}^{wf}\quad \bar{P}_{j,t+t_4}^{wf}\right] \tag{1}$$

$$T_{j,t}=\sum_{s=1}^{4}\operatorname{sign}\left(\bar{P}_{j,t+t_s}^{wf}-\bar{P}_{j,t+t_{s-1}}^{wf}\right) \tag{2}$$

where $\boldsymbol{P}_{j,Tre}^{WF}$ is the hourly predictive power dataset of WF j; $\bar{P}_{j,t+t_s}^{wf}$ is the predictive power at time $t+t_s$; t_s = 0, 15, 30, 45, 60 min ($s=0,1,\ldots,4$), which is the interval between sampling time and time t; and sign(x) is the signum function with three values, i.e., ±1, −1, and 0.

The categories of WFs are then determined based on the value of $T_{j,t}$. $T_{j,t}=\pm 4$ indicates a continuous increase or decrease in the output power over the next hour; while $-4<T_{j,t}<4$ indicates that the output power is in a state of fluctuation. To further quantify the power fluctuation, this paper introduces the statistical concepts of the range δ and threshold λ. In addition, the magnitude relationship between the two concepts is used as another clustering criterion. The calculation formula is given as:

$$\begin{cases}\delta_j=\max\left(\boldsymbol{P}_{j,Tre}^{WF}\right)-\min\left(\boldsymbol{P}_{j,Tre}^{WF}\right)\\ \lambda_j=P_j^N/100\end{cases} \tag{3}$$

where δ_j is the maximum power deviation in $\boldsymbol{P}_{j,Tre}^{WF}$; P_j^N is the installed capacity of WF j; and λ_j is derived from prior information.

The classification criteria for dynamic clustering are given in Table I.

TABLE I
Classification Criteria for Dynamic Clustering

$T_{j,t}$	Relationship between δ_j and λ_j	Clustering result
4	$\delta_j>\lambda_j$	Power-increase
	$\delta_j\le\lambda_j$	Power-steady
−4	$\delta_j>\lambda_j$	Power-decrease
	$\delta_j\le\lambda_j$	Power-steady
(−4, 4)	$\delta_j>\lambda_j$	Power-oscillatory
	$\delta_j\le\lambda_j$	Power-steady

In short, WFCs are classified into four subclusters: power-increase, power-decrease, power-steady, and power-oscillatory clusters, numbered ①-④, respectively. In addition, to prevent inconsistencies between the output trends of WF and dispatching command changes of WPC, the power regulation priorities of WFCs should be strictly defined, where the specific results are listed in Table II.

TABLE II
Power Regulation Priorities of WFCs

Dispatching command change trend	Power regulation priority
Increase	①>④>③>②
Decrease	②>④>③>①

B. Modeling for Formulation of Cluster Dispatching Plan

The core task of formulating cluster dispatching plan is to achieve the maximum wind power accommodation. Thus, the primary objective of this link is to minimize the curtailed wind power.

The output of WF is volatile due to random fluctuations in wind speed. According to the numerical values of the day-ahead predictive power of the WPC and the system dispatching command, two common operational modes can be obtained. ① Mode I: restricted output mode, in which the predictive power is greater than the dispatching command. ② Mode II: free generation mode, in which the predictive power is less than the dispatching command.

Then, based on different operating patterns, the reference values and control targets of active power are determined. The calculation process for the reference power is given as:

$$P_{t+\Delta t}^{ref}=\min\left\{P_{sys,t+\Delta t}^{dis},\sum_{i=1}^{M}\sum_{j=1}^{N}P_{ij,t+\Delta t}^{pre}\right\} \tag{4}$$

$$\Delta P_{t+\Delta t}=P^{ref}_{t+\Delta t}-\sum_{i=1}^{M}\sum_{j=1}^{N}P^{real}_{ij,t} \tag{5}$$

where $P^{ref}_{t+\Delta t}$ is the reference value at time $t+\Delta t$, and $\Delta t=1$ hour; $P^{dis}_{sys,t+\Delta t}$ is the system dispatching command; M is the number of WFCs; N is the total number of WFs in each WFC; $P^{pre}_{ij,t+\Delta t}$ is the predictive power of WF j in WFC i at time $t+\Delta t$; $P^{real}_{ij,t}$ is the actual output of WF j in WFC i at time t; and $\Delta P_{t+\Delta t}$ is the unbalanced power. The deviation between the reference value and actual output needs to be adjusted.

Finally, the WFCs participating in the adjustment and the total number C are obtained based on the power regulation priorities. The optimal dispatching models for the two modes are presented as follows.

1) Mode I: Restricted Output Mode

Under this working condition, the WPC tracks the instructions issued by the dispatching center. The main goal is to maximize the available wind energy and smooth out short-term fluctuations. The double-objective function of Mode I is given as:

$$\min J_{clu1}=\alpha_{i1}\sum_{i=1}^{M}\left(P^{opt}_{i,t+\Delta t}-\sum_{j=1}^{N}P^{pre}_{ij,t+\Delta t}\right)^2+\alpha_{i2}\sum_{i=1}^{C}\left(P^{opt}_{i,t+\Delta t}-\sum_{j=1}^{N}P^{real}_{ij,t}\right)^2 \tag{6}$$

where $P^{opt}_{i,t+\Delta t}$ is the optimized active power of WFC i at time $t+\Delta t$; and α_{i1} and α_{i2} are the weight coefficients of the performance indices, and $\alpha_{i1}+\alpha_{i2}=1$.

The main constraints are given as follows.

1) Constraint of dispatching plan

$$\sum_{i=1}^{M}P^{opt}_{i,t+\Delta t}=P^{dis}_{sys,t+\Delta t} \tag{7}$$

2) Power limitation of WFC

$$P^{\min}_{i}\le P^{opt}_{i,t+\Delta t}\le\sum_{j=1}^{N}P^{pre}_{ij,t+\Delta t}\le P^{\max}_{i} \tag{8}$$

where $P^{\min}_{i}$ and $P^{\max}_{i}$ are the output power limits of WFC i.

3) Constraint for ramping rate of WPC output

$$\left|\sum_{i=1}^{M}\left(P^{opt}_{i,t+\Delta t}-\sum_{j=1}^{N}P^{real}_{ij,t}\right)\right|\le C_{clu}P^{N}_{clu} \tag{9}$$

where P^{N}_{clu} is the total installed capacity of the WPC; and C_{clu} is the ramping rate limit of WPC output.

2) Mode II: Free Generation Mode

The only controlled objective of Mode II is to maximize the output wind power, and the objective function is give as:

$$\min J_{clu2}=\sum_{i=1}^{M}\left(P^{opt}_{i,t+\Delta t}-\sum_{j=1}^{N}P^{pre}_{ij,t+\Delta t}\right)^2 \tag{10}$$

In addition, (7) is modified as:

$$\sum_{i=1}^{M}P^{opt}_{i,t+\Delta t}\le P^{pre}_{clu,t+\Delta t} \tag{11}$$

where $P^{pre}_{clu,t+\Delta t}$ is the total predictive power of WFC i at time $t+\Delta t$.

The optimization results of $P^{opt}_{i,t+\Delta t}$ are regarded as the base values in the intra-day rolling dispatching.

C. Modeling for Plan Rolling Modification of Intra-cluster

To minimize the dispatching deviations caused by day-ahead predictive errors, the rolling modification link of intra-cluster plan fine-tunes the output plan of each WF at the WFC layer online. This is based on the power generation demand in the remaining period and the latest predictive results. The optimization horizon is 1 hour and the rolling cycle is 30 min. The optimization model considers the dynamic characteristics of power tracking, output power volatility, and wind power utilization as performance indices, with the target function given as:

$$\min J_{wfc}=\sum_{r=1}^{R}\left\{\left(P^{opt}_{i,t+\Delta t}-\sum_{j=1}^{N}P^{opt}_{ij,t+r\Delta t_1}\right)^2+\sum_{j=1}^{N}\left[\left(P^{opt}_{ij,t+r\Delta t_1}-P^{real}_{ij,t+(r-1)\Delta t_1}\right)^2+\left(P^{opt}_{ij,t+r\Delta t_1}-P^{pre}_{ij,t+r\Delta t_1}\right)^2\right]\right\} \tag{12}$$

where $P^{opt}_{ij,t+\Delta t_1}$ is the optimal reference power allocated to WF j at time $t+\Delta t_1$, and $\Delta t_1=30$ min; and $R=2$ is the rolling frequency. Only the optimization results of $r=1$ are considered and issued in each dispatching cycle.

To ensure the stability of the system, the rolling optimization must comply with the security constraints of the lower limit of predictive power, dispatching order tracking constraint, fluctuation restriction of grid-connected WF, and ramping rate limit.

$$\begin{cases}P^{pre}_{ij,t+\Delta t_1}\le k_{lp}P^{N}_{j}\Rightarrow P^{opt}_{ij,t+\Delta t_1}=P^{pre}_{ij,t+\Delta t_1}\\ \sum_{j=1}^{N}P^{opt}_{ij,t+\Delta t_1}\le P^{opt}_{i,t+\Delta t}\\ \left|P^{opt}_{ij,t+\Delta t_1}-P^{real}_{ij,t}\right|\le V_{wf}P^{N}_{j}\\ \left|\sum_{i=1}^{M}\sum_{j=1}^{N}P^{opt}_{ij,t+\Delta t_1}-\sum_{i=1}^{M}\sum_{j=1}^{N}P^{real}_{ij,t}\right|\le\tilde{C}_{clu}P^{N}_{clu}\end{cases} \tag{13}$$

where k_{lp} is the limit coefficient, and $k_{lp}=0.2$; V_{wf} is the output fluctuation limit of WF within 30 min and is set to be 7%; and $\tilde{C}_{clu}$ is the ramping rate limit of WPC output at a 30-min scale.

The calculation results of the intra-cluster layer are used as tracking targets for the wind power station.

D. Modeling for Optimization Allocation of WF

The optimization allocation of WF plays a crucial role in the APC within the cluster. Therefore, improving the control credibility of WFs is the primary goal of the dispatching link.

1) Dynamic Classification of WGs Based on Power Information and Operating Conditions

The response time and tracking accuracies of numerous WGs in a WF for dispatching commands are not the same. Besides, if the active power of WF is allocated directly, the corresponding distribution arithmetic will have problems such as dimension disasters and implementation difficulties. In this paper, based on the generation potential and actual operating status of the WG, the WGs are dynamically classified to prevent unreasonable power distribution and achieve the coordinated and complementary output of WGs in each WF.

The WG operates under three wind conditions according to real-time wind speed $v(t)$, i. e., ① low-wind-speed zone ($v_{ci} \le v(t) \le v_1$): the wind turbine operates in the maximum power point tracking (MPPT) mode; ② medium-wind-speed zone ($v_1 < v(t) < v_n$): the wind turbine operates at a constant rotation speed; and ③ high-wind-speed zone ($v_n \le v(t) \le v_{co}$): the wind turbine is in a constant-power state. Here, v_{ci} and v_{co} are the cut-in and cut-out wind speeds, respectively; v_1 is the wind speed corresponding to the rated rotation speed; and v_n is the rated speed. This paper uses the actual operating conditions of WGs as a classification criterion.

The second classification indicator is the power variation coefficient. For WG n in WTG m, the historical power at $t-\Delta t_3$ $P^{old}_{mn,t-\Delta t_3}$, the real-time output power $P^{real}_{mn,t}$ from the data monitoring system, and the predicted power $P^{pre}_{mn,t+\Delta t_3}$ at 5-min resolution are linearly fitted by the least-squares fitting, where $\Delta t_3 = 5$ min. Then, the power variation rate k_{mn} within 15 min is calculated and the power change coefficient β_{mn} is defined as:

$$\beta_{mn} = \frac{k_{mn}}{P_{mn,N}} \tag{14}$$

where $P_{mn,N}$ is the rated capacity of the wind turbine.

With reference to Technical Rule for Active Power Regulation and Control of Wind Farm [33], ±0.008 is chosen as the boundary value to determine the power variation trend. Based on the magnitudes of β_{mn} and ±0.008, the output of WG is categorized into three fluctuation scenarios: power-increase, power-stable, and power-decrease.

Finally, the start-up and shut-down units must be screened to reduce the dispatching frequency. Both types of WGs can be determined based on the relationship between $v(t)$, predicted wind speed $v_{pre}(t+\Delta t_2)$, v_{ci}, and v_{co}. If $v(t)$ and $v_{pre}(t+\Delta t_2)$ satisfy (15) and (16), the WG is in start-up and shut-down modes, respectively.

$$\begin{cases} v(t) < v_{ci} \\ v_{pre}(t+\Delta t_2) \ge v_{ci} \end{cases} \text{ or } \begin{cases} v(t) > v_{co} \\ v_{pre}(t+\Delta t_2) \le v_{co} \end{cases} \tag{15}$$

$$\begin{cases} v(t) \ge v_{ci} \\ v_{pre}(t+\Delta t_2) < v_{ci} \end{cases} \text{ or } \begin{cases} v(t) \le v_{co} \\ v_{pre}(t+\Delta t_2) > v_{co} \end{cases} \tag{16}$$

where $\Delta t_2 = 15$ min.

In summary, all WGs other than start-up and shut-down ones can be dynamically classified according to the selection and judgment processes, as shown in Fig. 3. The WF is divided into 11 clusters, and the classification results are listed in Table III. Combined with the WF dispatching values and WG grouping results, the required WTGs for dispatching and their total number g are obtained based on the priority ranking method.

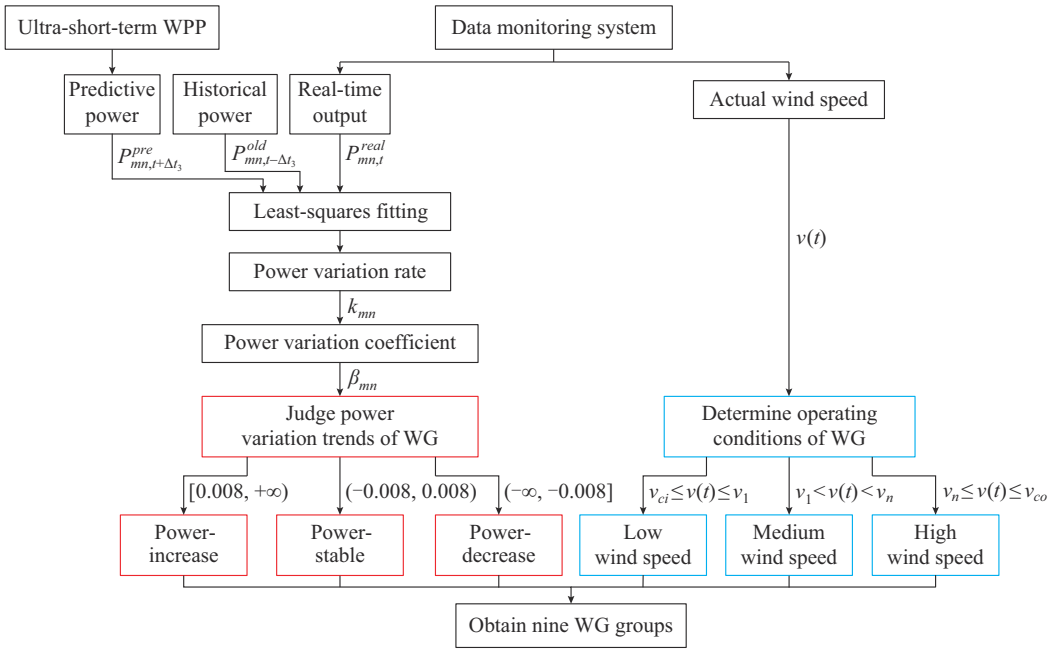

Fig. 3. Selection and judgement processes for dynamic classification of WGs.

TABLE III
CLASSIFICATION RESULTS OF WF

Cluster number	Classification result	Cluster number	Classification result
1	Low wind speed, power-increase	7	High wind speed, power-increase
2	Low wind speed, power-stable	8	High wind speed, power-stable
3	Low wind speed, power-decrease	9	High wind speed, power-decrease
4	Medium wind speed, power-increase	10	Start-up
5	Medium wind speed, power-stable	11	Shut-down
6	Medium wind speed, power-decrease		

2) Modelling for Optimal Power Allocation of WTG

The optimization time domain of this link is 30 min, and the rolling cycle is 15 min. The multi-objective optimization problem for the WF level is modeled as:

$$\begin{cases} \min J_{wf}=\left[P^{opt}_{ij,t+\Delta t_1}-\left(\sum_{m=1}^{g}\hat{P}^{opt}_{Rm,t+\Delta t_2}+\sum_{m=1}^{11-g}\hat{P}^{opt}_{Nm,t+\Delta t_2}\right)\right]^2+ \\ \qquad \sum_{m=1}^{g}\left(\hat{P}^{opt}_{Rm,t+\Delta t_2}-P^{real}_{Rm,t}\right)^2 \\ \text{s.t.}\ \ \sum_{m=1}^{g}\hat{P}^{opt}_{Rm,t+\Delta t_2}+\sum_{m=1}^{11-g}\hat{P}^{opt}_{Nm,t+\Delta t_2}\le P^{pre}_{j,t+\Delta t_2}\le P^{N}_{j} \\ \qquad \left|\frac{\hat{P}^{opt}_{Rm,t+\Delta t_2}-P^{real}_{Rm,t}}{P^{real}_{Rm,t}}\right|\le \hat{C}_{wf,j} \\ \qquad 0\le \hat{P}^{opt}_{Rm,t+\Delta t_2}\le P_{Rm,N} \end{cases} \tag{17}$$

where $\hat{P}^{opt}_{Nm,t+\Delta t_2}$ is the optimized output power of the non-regulated WTG m; $\hat{P}^{opt}_{Rm,t+\Delta t_2}$ is the optimal output power of WTG m involved in dispatching; $\hat{C}_{wf,j}$ is the 15-min climbing rate limit for WF j; and $P_{Rm,N}$ is the rated capacity of WTG m that must be adjusted.

E. Modeling for Grouping Coordinated Control of WTG

After the WF allocates reference active power values to each WTG, the WTG layer performs the rolling optimization every 5 min and sends the optimized results to the bottom layer. The bottom layer is intended to suppress frequent changes in the output of WG to smooth WF operation. The objective function is expressed as:

$$\min J_{wt}=\sum_{r=1}^{3}\sum_{n=1}^{K}\left(P^{opt}_{mn,t+r\Delta t_3}-P^{real}_{mn,t+(r-1)\Delta t_3}\right)^2 \tag{18}$$

where r is the index of rolling counter; $P^{opt}_{mn,t+r\Delta t_3}$ is the optimal power of WG n in WTG m at time $t+r\Delta t_3$, and $\Delta t_3=5$ min; and K is the total number of WGs in WTG m. In addition, this link complies with the following constraints.

$$\begin{cases} \sum_{r=1}^{3}P^{opt}_{mn,t+r\Delta t_3}=\hat{P}^{opt}_{m,t+\Delta t_2} \\ 0\le P^{opt}_{mn,t+r\Delta t_3}\le P_{mn,N} \\ \left|P^{opt}_{mn,t+r\Delta t_3}-P^{real}_{mn,t+(r-1)\Delta t_3}\right|\le \hat{C}_{wt,n}P^{real}_{mn,t} \end{cases} \tag{19}$$

where $\hat{P}^{opt}_{m,t+\Delta t_2}$ is the 15-min allocation result for WTG m; and $\hat{C}_{wt,n}$ is the ramping rate limit of WG n.

F. Modeling for Real-time Adjustment of Single-machine Power

To minimize the output deviation of the WG from the expected value issued by the upper level, the real-time adjustment link of single-machine power regulates the active power of WG with a 1-min control cycle. This step is based on the target power, which is updated every 5 min. To simplify the calculation, the objective function is represented by the square of the dispatching deviation:

$$\min J_{err}=(P^{opt}_{mn,t+\Delta t_4}-P^{real}_{mn,t})^2 \tag{20}$$

s.t.

$$\begin{cases} P^{opt}_{mn,t+\Delta t_4}\le P^{opt}_{mn,t+\Delta t_3} \\ \left|\frac{P^{opt}_{mn,t+\Delta t_4}-P^{real}_{mn,t}}{P^{real}_{mn,t}}\right|\le \hat{C}_{wt,n} \\ 0\le P^{opt}_{mn,t+\Delta t_4}\le P_{mn,N} \end{cases} \tag{21}$$

where $\Delta t_4=1$ min.

In addition, the constraints include the dispatching target tracking, power limit of WG output, and climbing rate limit of WG output.

IV. Detailed Formulation of MPC for WPC Active Power

MPC is a model-based closed-loop control approach for rolling optimization in a finite-time domain. The control core consists of three parts: predictive model, rolling optimization, and feedback correction. To better accommodate the stratified coordination control strategy, this paper proposes more refined models for these three links.

A. Combined WPP Method Based on CMMEDAN-WT-LSSVM

The collaboration between WPP and cluster coordination control is an effective way to diminish the impact of wind power uncertainty. However, due to the complex and variable meteorological conditions of WFCs, the applicability of a single predictive model is limited. By contrast, the integration of multiple methods with complementary advantages can further improve the predictive precision. Therefore, this paper adopts a fusion-based combined predictive method for wind power.

The entire predictive process consists of two key links: input data optimization and predictive model formulation.

1) Input data optimization. The wind power is characterized by strong randomness and rapid fluctuations. For data validity and predictive accuracy, the pre-processing of the sample data is essential. Wavelet decomposition (WD) and empirical mode decomposition (EMD) are commonly used in the decomposition of non-linear non-stationary time series, but both have some limitations. As an improved signal decomposition algorithm, CCEMDAN can overcome the shortcomings of the poor adaptability of wavelet basis functions, mode mixing, and the endpoint effect of EMD. To further eliminate the noise residuals, we introduce the WT method to denoise the decomposed signals. In short, this paper uses the joint denoising approach CEEMDAN-WT to optimize historical input data. First, the original wind power time series is decomposed into several intrinsic mode function (IMF) components using the CEEMDAN algorithm. The high-frequency (HF) random components and low-frequency (LF) trend components are then screened using the correlation coefficient. The screening results are checked using the variance contribution rate. Finally, the WT method is used to denoise the HF IMFs.

2) Predictive model formulation. Considering the structural complexity of the predictive model and the rapidity of dis-

patching control, this paper selects the LSSVM model because of its high generalization ability. The time-series prediction based on LSSVM not only ensures the precision, but also improves the solving speed. The environmental parameters of wind speed, wind direction, temperature, and humidity are combined with the denoised HF signals and the raw LF components to form training sets that are input into proper LSSVM models. The predictive results for each component are obtained after training and testing. The final predictive power is then acquired by superposition reconstruction. The flow of the WPP strategy is shown in Fig. 4.

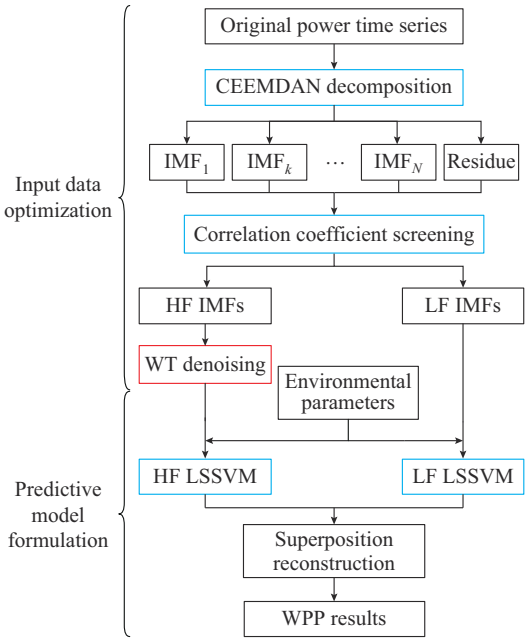

Fig. 4. Flow of WPP strategy.

B. Hierarchical Rolling Optimization Based on QDMC

For simplicity, high computational efficiency, and strong robustness, the dynamic matrix control (DMC) has become one of the most commonly-used predictive control algorithms in industrial processes. Quadratic dynamic matrix control (QDMC), being an extension of DMC, mainly obtains the best performance in satisfying the constraints by solving quadratic programming (QP) problems online. Because APD can be transformed into a QP problem, this paper uses the QDMC algorithm for hierarchical rolling optimization to solve the aforementioned dispatching problems. The optimized dispatching power and the power to be regulated are output-variable and input-control-variable, respectively. Based on the property of proportional superposition, the relationship between them can be expressed as:

$$\boldsymbol{P}^{opt}(t+\Delta t)=\boldsymbol{P}^{real}(t)+\boldsymbol{A}\Delta\boldsymbol{P}^{opt}(t+\Delta t) \tag{22}$$

where $\boldsymbol{P}^{real}(t)$ is the matrix of real output; $\boldsymbol{P}^{opt}(t+\Delta t)$ and $\Delta\boldsymbol{P}^{opt}(t+\Delta t)$ are the matrices of optimal output power and the APC increment, respectively; and $\boldsymbol{A}$ is the dynamic matrix, which is a $P\times M$ matrix composed of the response coefficients a_p:

$$\boldsymbol{A}=\begin{bmatrix} a_1 & 0 & \cdots & 0 \\ a_2 & a_1 & \cdots & 0 \\ \vdots & \vdots & & \vdots \\ a_M & a_{M-1} & \cdots & a_1 \\ a_{M+1} & a_M & \cdots & a_2 \\ \vdots & \vdots & & \vdots \\ a_P & a_{P-1} & \cdots & a_{P-M+1} \end{bmatrix} \tag{23}$$

where the subscript P is the optimization time domain; the subscript M is the rolling control horizon; and $a_p=1$ ($p=1,2,\ldots,P$).

To maintain the consistency in the model description, both the objective function and constraints are vectorized into the standard QP form. Taking the formulation of cluster dispatching plan as an example, the mathematical derivation processes of the objective function transformation in vector form in the two operation modes are given as follows.

1) Mode I – Restricted Output Mode

$$\begin{aligned}\min J_{clu1}(t)=&\left\|\boldsymbol{P}_{WFC}^{real}(t)+\boldsymbol{A}\Delta\boldsymbol{P}_{WFC}^{opt}(t+\Delta t)-\boldsymbol{P}_{WFC}^{pre}(t+\Delta t)\right\|_{\boldsymbol{Q}_1}^2+\\ &\left\|\boldsymbol{P}_{WFC}^{real}(t)+\boldsymbol{A}\Delta\boldsymbol{P}_{WFC}^{opt}(t+\Delta t)-\boldsymbol{P}_{WFC}^{real}(t)\right\|_{\boldsymbol{Q}_2}^2+\left\|\Delta\boldsymbol{P}_{WFC}^{opt}(t+\Delta t)\right\|_{\boldsymbol{R}_1}^2=\\ &\left\|\boldsymbol{P}_{WFC}^{real}(t)+\boldsymbol{A}\Delta\boldsymbol{P}_{WFC}^{opt}(t+\Delta t)-\boldsymbol{P}_{WFC}^{pre}(t+\Delta t)\right\|_{\boldsymbol{Q}_1}^2+\\ &\left\|\boldsymbol{A}\Delta\boldsymbol{P}_{WFC}^{opt}(t+\Delta t)\right\|_{\boldsymbol{Q}_2}^2+\left\|\Delta\boldsymbol{P}_{WFC}^{opt}(t+\Delta t)\right\|_{\boldsymbol{R}_1}^2\end{aligned} \tag{24}$$

where the subscript *WFC* represents the corresponding values of WFC; the diagonal matrix $\boldsymbol{Q}_i$ ($i=1,2,3$) is the error weight matrix; $\boldsymbol{R}_j$ ($j=1,2$) is the control weight matrix; and the control increment matrix $\Delta\boldsymbol{P}_{WFC}^{opt}(t+\Delta t)$ can be obtained by solving QP problems online.

2) Mode II – Free Generation Mode

$$\begin{aligned}\min J_{clu2}(t)=&\left\|\boldsymbol{P}_{WFC}^{real}(t)+\boldsymbol{A}\Delta\boldsymbol{P}_{WFC}^{opt}(t+\Delta t)-\boldsymbol{P}_{WFC}^{pre}(t+\Delta t)\right\|_{\boldsymbol{Q}_3}^2+\\ &\left\|\Delta\boldsymbol{P}_{WFC}^{opt}(t+\Delta t)\right\|_{\boldsymbol{R}_2}^2\end{aligned} \tag{25}$$

C. Error Analysis and Feedback Correction

The main causes of short-term dispatching errors include predictive errors, system control performance, and power fluctuations derived from the random and intermittent nature of wind speeds.

To minimize the APC deviations and ensure that the optimal output of WPC is more realistic, this paper incorporates a feedback correction link in the WG layer. The response of WG to the power control is rapid, and the feedback correction cycle of the WG itself is extremely short. As a result, the WG can take the actual current output as the initial value of rolling optimization in the next minute and directly feed it back to (24). The real-time correction is then performed through the rolling optimization. Simultaneously, the predictive errors per minute are obtained and aggregated based on the predictive output and monitored power data. The upper-layer predictive power is corrected using a linear weighting method. Finally, the correction results are fed back to the WF layer to form a closed-loop control. The mathematical formula for feedback correction is expressed as:

$$\hat{P}_{t+\Delta t_2}^{pre}=P_t^{pre}+\boldsymbol{WE} \tag{26}$$

$$\begin{cases} \boldsymbol{W}=\begin{bmatrix} w_{t+1} & w_{t+2} & \cdots & w_{t+\Delta t_2} \end{bmatrix} \\ \boldsymbol{E}=\begin{bmatrix} e_{t+1} & e_{t+2} & \cdots & e_{t+\Delta t_2} \end{bmatrix}^{\mathrm{T}} \\ e_{t+k}=P_{t+k}^{real}-P_{t}^{pre} \quad k=1,2,\ldots,\Delta t_2 \end{cases} \tag{27}$$

where $\boldsymbol{W}$ and $\boldsymbol{E}$ are the correction and error vectors, respectively; and the correction coefficient w_{t+k} $(k=1,2,\ldots,\Delta t_2)$ is considered to decrease with time.

V. Example Testing

A. Test System

The feasibility and effectiveness of the proposed HCCC strategy are verified using typical daily data from a WPC in southeast China. The simplified wiring diagram of the target WPC is illustrated in Fig. 5. The WPC contains three large-scale WFs, and the specific parameters of each WF are listed in Table IV. To guarantee the security and economy of the system connected with wind power, this paper assumes that the technical minimum output of the WFs and the regulation lower limit of the WGs are 15% of their respective installed capacities.

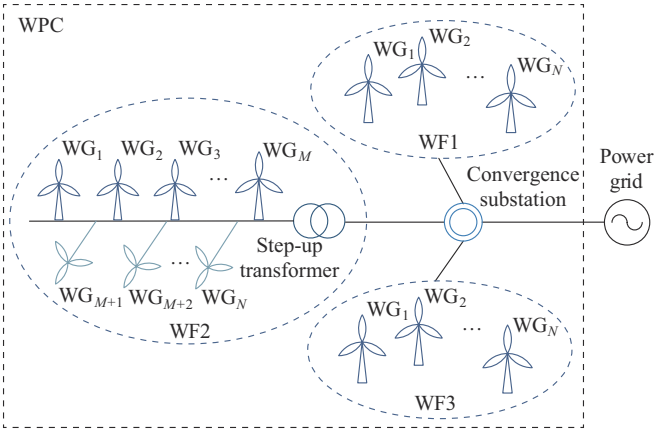

Fig. 5. Simplified wiring diagram of target WPC.

TABLE IV
Specific Parameters of Each WF

WF No.	Installed capacity (MW)	Low predictive constraint (MW)	Adjustment lower limit (MW)
WF1	400	80	60
WF2	300	60	45
WF3	400	80	60

The simulation calculation is based on MATLAB R2020b, and the computer is configured as an Intel Core™ i7-1165G7 CPU (2.80 GHz) with 16 GB of RAM under Windows 10.

B. Evaluation Testing of Combined Predictive Model

To assess the rationality of the proposed combined predictive model, the obtained predictive results are compared with those of the complex particle swarm optimization LSSVM (PSO-LSSVM) model and simple autoregressive moving average (ARMA) model.

To fully capture the WPC information, the continuous and complete raw data from January 17 to 23, 2022, with a 15-min time resolution are selected as the sample sequences in this paper. The day-ahead predictive curves and evaluation indices of the WPC on January 23 under different predictive models are presented in Fig. 6 and Table V, respectively.

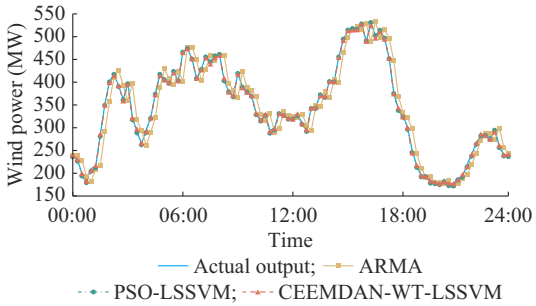

Fig. 6. Actual output of WPC and power prediction under different predictive models.

TABLE V
Evaluation Indices of WPC

Predictive model	Time (s)	MAE	MAPE (%)	RMSE
ARMA	49.50	14.38	6.80	19.11
PSO-LSSVM	30.71	2.91	1.07	3.44
CEEMDAN-WT-LSSVM	15.43	2.56	0.82	3.16

Note: MAE, MAPE, and RMSE are short for mean absolute error, mean absolute percentage error, and root mean square error, respectively.

Figure 6 shows that the combined predictive model CEEMDAN-WT-LSSVM outperforms the ARMA. In particular, when the wind speed fluctuates frequently, the predictive accuracy is significantly improved. The predictive effect is similar to that of the PSO-LSSVM algorithm.

As shown in Table V, the proposed combined predictive model clearly runs faster than the other two models. Although the PSO algorithm improves the predictive performance by optimizing the model parameters, the iterative optimization process increases the time complexity of the algorithm, which is unfavorable for realizing fast prediction. Overall, the proposed predictive model is more conducive to coordinating APD.

C. Simulation Analysis of HCCC Strategy

To analyze the daily output characteristics of the selected WPC, we choose the measured data from January 1 to 31, 2022, with a sampling interval of 15 min. Figure 7 depicts the minute-level output curves of the three WFs.

The wind power generation status is strongly correlated with wind resources, and the outputs of WFs are variable. For a more comprehensive and reliable study of power dynamic dispatching, we quantify the daily output of the WPC based on the wind generation rate (actual output divided by installed capacity). With 1/3 and 2/3 as the boundaries, the actual operating states of WPC are delineated as low, medium, and high wind-energy generation. Then, according to the proportion of each state, three typical daily operation scenarios are obtained, i.e., low-, medium-, and high-output scenarios.

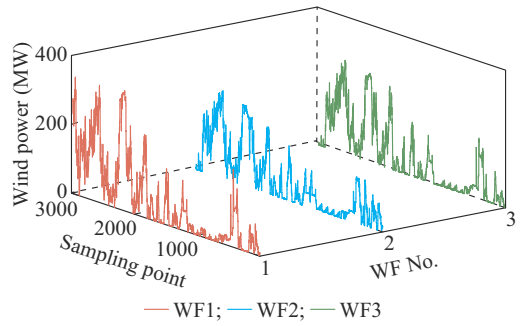

Fig. 7. Minute-level output curves of three WFs.

In addition, to study the seasonal variation characteristics of the WPC output, a statistical analysis is conducted on the monthly average output of WFs, as shown in Fig. 8. The results reveal that the high-output scenarios of WFs are mainly concentrated in winter and spring, whereas the low-output scenarios are mostly in summer. Accordingly, the measured power data in summer and winter are used to simulate the low- and high-output scenarios for testing the adaptability of the proposed strategy to changing external environments.

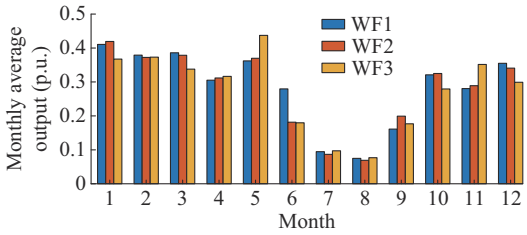

Fig. 8. Monthly average output of three WFs.

Figure 9 shows the APD control results of WPC in the high- and low-output scenarios. The optimization effects of the formulation of cluster dispatching plan and rolling modification of intra-cluster plan are illustrated.

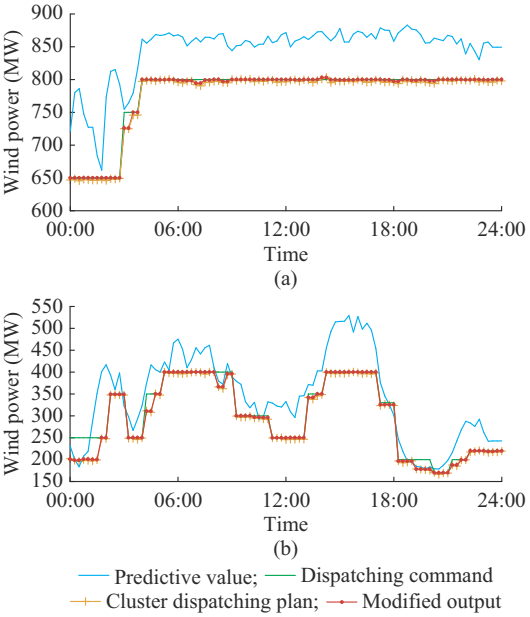

Fig. 9. APD control results of WPC in different scenarios. (a) High-output scenario. (b) Low-output scenario.

As shown in Fig. 9(a), in the high-output scenario, the equivalent load is relatively small and the WPC often runs in the restricted output mode. Therefore, on the premise of satisfying the given power limits of the grid, the main objective is to maximize the output of WPC. Through the multi-time-space coordination, the output of WF is optimized to track the dispatching value.

Table VI shows the comparison results of different dispatching control links. Tracking accuracy is measured by the RMSE between the output power and dispatching commands. In addition, the fluctuation characteristic is quantitatively assessed by the average power variation rate and the times of fluctuation overlimit. Clearly, after the rolling modification is introduced into the reference power, the WFs perform better in tracking the dispatching plan of the WFC, inhibiting short-term fluctuations, and maximizing the output.

TABLE VI
COMPARISON RESULTS OF DIFFERENT DISPATCHING CONTROL LINKS

Dispatching control link	Wind power utilization rate (%)	Dispatching deviation (%)	Power variation rate (%)	Limit crossing times
Formulation of cluster dispatching plan	92.77	–1.66	0.59	3
Formulation of cluster dispatching plan + rolling modification of intra-cluster plan	94.55	–0.91	0.15	0

In the low-output scenarios, e.g., the period of 00:00-01:30, as shown in Fig. 9(b), the system dispatching orders are higher than the predictive power of WPC. To maximize the wind power utilization rate, the WPC runs in the free generation mode. The day-ahead predictive power is taken as the reference value to rationalize the output power. For most of the remaining time, the cluster is in a restricted output state. It can be verified that the dispatching performance is improved with finer spatiotemporal granularity.

The newly added rolling modification link of intra-cluster plan can correct the improper power allocation caused by the upper-layer control based on the latest predictive information. It also combines safety constraints such as the 30-min volatility restriction to fine-tune the planned power output.

Because low-speed wind accounts for a large proportion, it is necessary to further discuss the dispatching results of the low-output case. To validate the rationality of the proposed dynamic clustering strategy for WFs, this paper analyzes the active power regulation behavior of four WFCs during the period of 00: 00-06: 00. The wind power output variations of each subcluster are shown in Fig. 10. During this period, the anti-peak shaving characteristics of the wind power output are more obvious. However, WFCs could still schedule active power in strict accordance with priority.

To validate the APC performance of individual WFs, the HCCC strategy proposed in this paper is compared with conventional active power allocation methods including FPA and VPA methods. The FPA method allocates power com-

mands to each WF based on the installed capacity, whereas the VPA method performs proportional distribution control based on the predictive WF power. Figure 11 shows the APC effects of different methods on WF1-WF3.

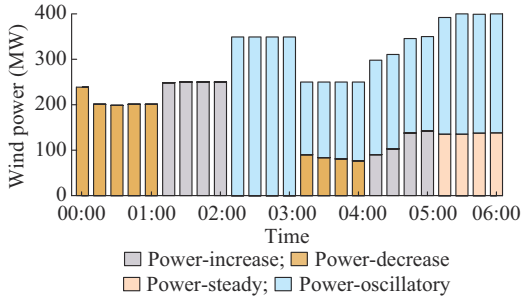

Fig. 10. Wind power output variations of each subcluster.

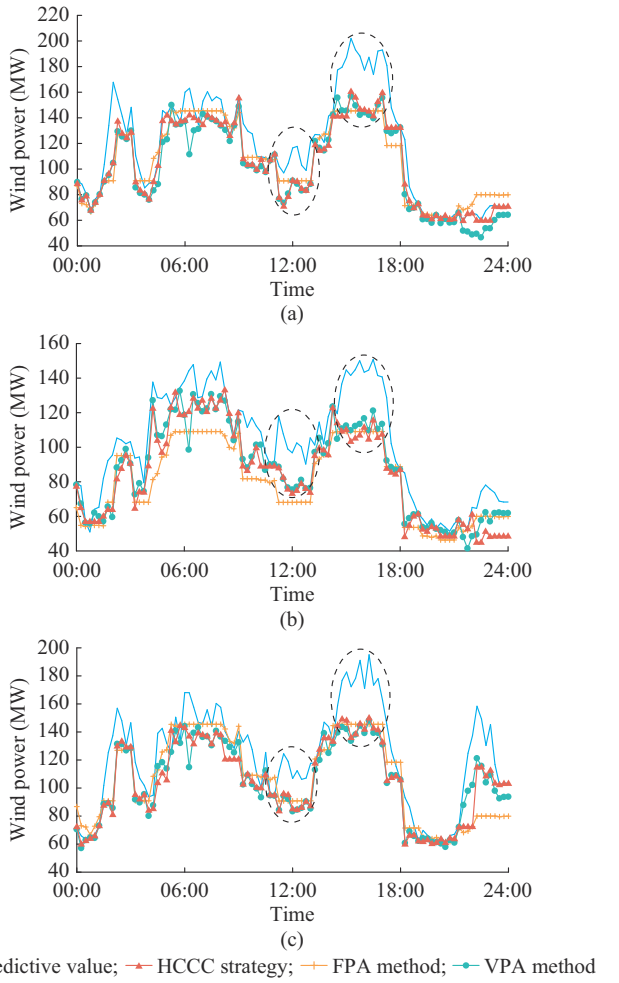

Fig. 11. APC effects of different methods on three WFs. (a) WF1. (b) WF2. (c) WF3.

A comparative analysis of Fig. 11 indicates that the modulation effect of the FPA method on the active power is generally worse than those of the other two methods. The FPA method fails to consider the predictive information within the control period, resulting in an unjustified distribution of the dispatching power to WFs. Taking WF2 as an example, under the continuously high predictive power from 05:00 to 09:00, the FPA method does not issue more dispatching power, leading to more wind curtailment. By contrast, the VPA method increases the wind power accommodation rate to some extent. In addition, because the control time domain of the HCCC strategy coincides with the ultra-short-term predictive cycle, it could respond quickly to power adjustment demands and accurately allocate power.

To evaluate the economy and security of the HCCC strategy, we analyze the output volatility and wind power accommodation rate based on the power variation and wind curtailment rates. The results in Table VII show that the wind curtailment rate of the HCCC strategy is the lowest among the three methods. The HCCC strategy can track the predictive curve as much as possible while simultaneously coordinating the outputs of WFs to improve the power generation utilization rate. Figure 11 shows that the outputs of the three WFs deviate significantly from the predictive values during the periods of 11:00-13:00 and 15:00-17:00 (circled by dashed lines). This is because the output of WF is limited by the power reduction instructions issued as a result of the decreasing load demand. In addition, the calculation results of the power variation rate reveal that the application of HCCC strategy makes the outputs of WFs smoother, and alleviates the shock to the grid caused by rapid and violent fluctuations.

TABLE VII
COMPARISON RESULTS OF DIFFERENT CONTROL METHODS

WF No.	Power variation rate (%)			Wind curtailment rate (%)		
	FPA	VPA	HCCC	FPA	VPA	HCCC
WF1	0.0178	0.0666	0.0464	4.1633	3.4076	2.8122
WF2	0.0178	0.1106	0.0571	7.0527	5.5169	4.6934
WF3	0.0178	0.0804	0.0604	4.3381	4.3937	3.7816

Taking WF2 as an example, we discuss the coordination and complementarity of in-station WG output. WF2 has a total installed capacity of 300 MW, including four 25 MW WGs and five 40 MW WGs. Table VIII presents the assessment indices for intra-day dispatching plan of WF2, where the RMSE characterizes the control deviation of grouping control; and N_s and N_v are the start-stop times of WGs and the fluctuation frequency of WG dispatching, respectively.

TABLE VIII
ASSESSMENT INDICES OF DIFFERENT CONTROL METHODS ON WF2

Method	RMSE (%)	N_s	N_v
FPA	6.3167	48	63
VPA	4.8754	65	56
HCCC	2.5336	0	44

Compared with FPA and VPA methods, the RMSEs of the HCCC strategy decrease by 59.89% and 48.03%, respectively. This shows that the proposed HCCC strategy guarantees the APC accuracy of WFs at a high time resolution (15 min or less). In addition, the traditional distribution method is prone to frequent unit starting and stopping during the low

predictive output stage (e.g., 21:30-22:00 for WF2). By contrast, the grouping coordinated control can adjust the output of WG in a targeted manner based on ultra-short-term dispatching changes and power regulation capabilities of WG. This method also imposes start-stop constraints to avoid over-regulation of power-decrease units. Furthermore, the HCCC strategy can effectively reduce the action frequency of some WGs and improve the operation stability of the WF.

Finally, the effectiveness of real-time control with a 1-min resolution at the WG layer is analyzed. Figure 12 shows the active power regulation results of WTGs within 5 min between two adjacent rolling optimizations at the grouping control layer. According to the difference between the actual output at 05:40 and the planned output at the optimization moment 05:45, the power-decrease units with high wind speed preferentially execute the power reduction command, whereas others keep their current outputs unchanged. As can be observed, WTG9 reaches the lower regulation limit at 05:42. The power-decrease WGs with medium wind speed follow immediately with power curtailment and achieve the target at 05:44. Through the fine control of WGs, the WF can achieve a dynamic power balance and smooth output.

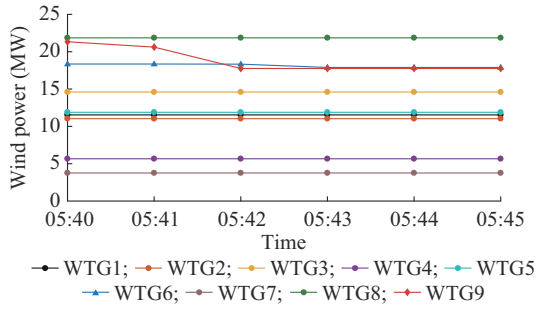

Fig. 12. Active power regulation results of WTGs within 5 min.

Figure 13 presents the local feedback correction results of WF2 during the ultra-short-term WPP. In this paper, the correction performance is studied to verify the validity of this feedback correction method. The modified predictive output is closer to the actual operating curve. Table IX presents the evaluation indices of the predictive results before and after correction. It can be observed that the predictive model combined with error correction can efficiently improve the predictive precision and provide a data basis for the fine control of the WPC.

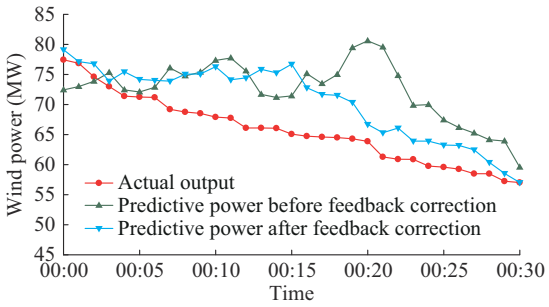

Fig. 13. Local feedback correction results of WF2 during ultra-short-term WPP.

TABLE IX
EVALUATION INDICES OF PREDICTIVE RESULTS BEFORE AND AFTER CORRECTION

Status	MAE	MAPE (%)	RMSE
Before correction	4.7835	7.3270	5.5954
After correction	7.4397	11.6390	8.6403

VI. CONCLUSION

To suppress the uncertainty caused by wind power integration in power system dispatching, a strategy based on MPC and improved multi-time-scale is proposed in this paper. Through the analysis and simulation verification, the following conclusions are obtained.

1) The combined predictive method CMMEDAN-WT-LSSVM based on input data optimization rapidly provides up-to-date predictive data. It not only meets the requirements of model dependability and high predictive precision but also ensures the smooth progress of APD control. In addition, the fast prediction contributes to a dynamic balance between the complexity of APD and the rapidity of real-time control.

2) Further refinement of the short-term dispatching time scale can effectively weaken the adverse effects of day-ahead predictive errors, shorten the response time to dispatching plans, and improve the power tracking accuracy and rolling control precision.

3) The stratified rolling optimization based on the QDMC algorithm takes the active power to be adjusted as a control variable and performs active power regulation on a layer-by-layer basis. In addition, this paper narrows the real-time control cycle to 1 min and introduces a feedback correction link to correct the dispatching results. This improved scheme minimizes the control deviations and simultaneously reduces the fluctuation frequency of WG regulation to enhance the economics of the system.

REFERENCES

[1] X. Chen, X. Wu, and K. Y. Lee, "The mutual benefits of renewables and carbon capture: achieved by an artificial intelligent scheduling strategy," *Energy Conversion and Management*, vol. 233, pp. 113856-113870, Apr. 2021.

[2] Z. Chen, "Wind power in modern power systems," *Journal of Modern Power Systems and Clean Energy*, vol. 1, no. 1, pp. 2-13, Jun. 2013.

[3] B. Mohandes, M. S. E. Moursi, N. Hatziargyriou *et al.*, "A review of power system flexibility with high penetration of renewables," *IEEE Transactions on Power Systems*, vol. 34, no. 4, pp. 3140-3155, Jul. 2019.

[4] M. Andrychowicz, B. Olek, and J. Przybylski, "Review of the methods for evaluation of renewable energy sources penetration and ramping used in the Scenario Outlook and Adequacy Forecast 2015. Case study for Poland," *Renewable and Sustainable Energy Reviews*, vol. 74, pp. 703-714, Jul. 2017.

[5] H. Pandžić, Y. Dvorkin, T. Qiu *et al.*, "Toward cost-efficient and reliable unit commitment under uncertainty," *IEEE Transactions on Power Systems*, vol. 31, pp. 970-982, Mar. 2016.

[6] G. Ren, J. Liu, J. Wan *et al.*, "Overview of wind power intermittency: impacts, measurements, and mitigation solutions," *Applied Energy*, vol. 204, no. 15, pp. 47-65, Oct. 2017.

[7] L. Ye, R. Chen, Z. Li *et al.*, "Stratified progressive predictive control strategy for multi-objective dispatching active power in wind farm," *Proceedings of the CSEE*, vol. 36, no. 23, pp. 6327-6336, Dec. 2016.

[8] X. Gao, K. Meng, Z. Dong *et al.*, "Cooperation-driven distributed control scheme for large-scale wind farm active power regulation," *IEEE Transactions on Energy Conversion*, vol. 32, no. 3, pp. 1240-1250,

Sept. 2017.
[9] Y. Yang, W. Wu, B. Wang *et al*., "Optimal decomposition of stochastic dispatch schedule for renewable energy cluster," *Journal of Modern Power Systems and Clean Energy*, vol. 9, no. 4, pp. 711-719, Jul. 2021.
[10] A. Cerejo, S. J. P. S. Mariano, P. M. S. Carvalh *et al.*, "Hydro-wind optimal operation for joint bidding in day-ahead market: storage efficiency and impact of wind forecasting uncertainty," *Journal of Modern Power Systems and Clean Energy*, vol. 8, no. 1, pp. 142-149, Jan. 2020.
[11] H. Zang, L. Cheng, T. Ding *et al.*, "Day-ahead photovoltaic power forecasting approach based on deep convolutional neural networks and meta learning," *International Journal of Electrical Power & Energy Systems*, vol. 118, pp. 105790-105805, Jun. 2020.
[12] X. Teng, Z. Gao, B. Zhu *et al.*, "Requirements analysis and key technologies for automatic generation control for smart grid dispatching and control systems," *Automation of Electric Power Systems*, vol. 39, no. 1, pp. 81-87, Jan. 2015.
[13] J. Zhai, J. Ren, M. Zhou *et al.*, "Multi-time scale fuzzy chance constrained dynamic economic dispatch model for power system with wind power," *Power System Technology*, vol. 40, no. 4, pp. 1094-1099, Apr. 2016.
[14] Z. Li, W. Wu, B. Zhang *et al.*, "Adjustable robust real-time power dispatch with large-scale wind power integration," *IEEE Transactions on Sustainable Energy*, vol. 6, no. 2, pp. 357-368, Apr. 2015.
[15] Z. Bao, Q. Zhou, Z. Yang *et al.*, "A multi time-scale and multi energy-type coordinated microgrid scheduling solution-part I: model and methodology," *IEEE Transactions on Power System*, vol. 30, no. 5, pp. 2257-2266, Sept. 2015.
[16] H. Wu, I. Krad, A. Florita *et al.*, "Stochastic multi-timescale power system operations with variable wind generation," *IEEE Transactions on Power System*, vol. 32, no. 5, pp. 3325-3337, Sept. 2017.
[17] H. Qiu, W. Gu, Y. Xu *et al.*, "Multi-time-scale rolling optimal dispatch for AC/DC hybrid microgrids with day-ahead distributionally robust scheduling," *IEEE Transactions on Sustainable Energy*, vol. 10, no. 4, pp. 1653-1663, Oct. 2019.
[18] M. Song, W. Sun, M. Shahidehpour *et al.*, "Multi-time scale coordinated control and scheduling of inverter-based TCLs with variable wind generation," *IEEE Transactions on Sustainable Energy*, vol. 12, no. 1, pp. 46-57, Jan. 2021.
[19] B. Zhang, J. Chen, and W. Wu, "Active hierarchical model predictive control method for large-scale wind power connected to power grid," *Automation of Electric Power Systems*, vol. 38, no. 9, pp. 6-14, May 2014.
[20] P. Lu, L. Ye, Y. Tang *et al.*, "Multi-time scale active power optimal dispatch in wind power cluster based on model predictive control," *Proceedings of the CSEE*, vol. 39, no. 22, pp. 6572-6582, Nov. 2019.
[21] Y. Ma, Y. Yu, and Z. Mi, "Accommodation of curtailed wind power by electric boilers equipped in different locations of heat-supply network for power system with CHPs," *Journal of Modern Power Systems and Clean Energy*, vol. 9, no. 4, pp. 930-939, Jul. 2021.
[22] X. Dou, J. Wang, Z Wang *et al.*, "A dispatching method for integrated energy system based on dynamic time-interval of model predictive control," *Journal of Modern Power Systems and Clean Energy*, vol. 8, no. 5, pp. 841-852, Sept. 2020.
[23] C. Wang, Z. Du, Y. Ni *et al.*, "Coordinated predictive control for wind farm with BESS considering power dispatching and equipment aging," *IET Generation Transmission & Distribution*, vol. 12, no. 10, pp. 2406-2414, Mar. 2018.
[24] W. R. Sultana, S. K. Sahoo, S. Sukchai *et al.*, "A review on state-of-the-art development of model predictive control for renewable energy applications," *Renewable and Sustainable Energy Reviews*, vol. 76, pp. 391-406, Sept. 2017.
[25] A. Koerber and R. King, "Combined feedback-feedforward control of wind turbines using state-constrained model predictive control," *IEEE Transactions on Control Systems Technology*, vol. 21, no. 4, pp. 1117-1128, Jul. 2013.
[26] S. Riverso, S. Mancini, F. Sarzo *et al.*, "Model predictive controllers for reduction of mechanical fatigue in wind farms," *IEEE Transactions on Control Systems Technology*, vol. 25, no. 2, pp. 535-549, Mar. 2017.
[27] J. Zhai, M. Zhou, S. Dong *et al.*, "MPC-based two-stage rolling power dispatch approach for wind-integrated power system," *Journal of Electrical Engineering & Technology*, vol. 13, no. 2, pp. 648-658, Mar. 2018.
[28] D. Zhu and G. Hug, "Decomposed stochastic model predictive control for optimal dispatch of storage and generation," *IEEE Transactions on Smart Grid*, vol. 5, no. 4, pp. 2044-2053, Jul. 2014.
[29] G. Li, Y. Ren, Z. Wang *et al.*, "Double-layer feedback control method for synchronized frequency regulation of PMSG-based wind farm," *IEEE Transactions on Sustainable Energy*, vol. 12, no. 4, pp. 2423-2435, Oct. 2021.
[30] S. Huang, Q. Wu, Y. Guo *et al*., "Bi-level decentralized active and reactive power control for large-scale wind farm cluster," *International Journal of Electrical Power & Energy Systems*, vol. 111, pp. 201-215, Oct. 2019.
[31] Y. Lin, C. Zhang, Y. Tang *et al*., "Active power stratification predictive control approach for wind power cluster with multiple temporal and spatial scales coordination," *Proceedings of the CSEE*, vol. 38, no. 13, pp. 3767-3780, Jul. 2018.
[32] Y. Lin, Y. Tang, W. Zhong *et al*., "Hierarchical model predictive control strategy based on dynamic active power dispatch for wind power cluster integration," *IEEE Transactions on Power Systems*, vol. 34, no. 6, pp. 4617-4629, Nov. 2019.
[33] *Technical Rule for Active Power Regulation and Control of Wind Farm*, NB/T 31110-2017, 2017.

Ying Zhu received the B.E. degree in electrical engineering and its automation from Southeast University, Nanjing, China, in 2008, and the Ph.D. degree in electrical engineering from Southeast University, in 2014. She is currently working as an Associate Professor with the College of Energy and Electrical Engineering, Hohai University, Nanjing, China. Her research interests include renewable power generation and its forecasting, and integration of renewable energies into power systems.

Yanan Zhang received the B.E. degree in electrical engineering and its automation from Hohai University, Nanjing, China, in 2020. She is currently pursuing the M. Sc. degree in electric engineering from Hohai University. Her research interests include intermittent new energy generation and grid-connected operation control, optimal scheduling of power system, and renewable energy generation forecasting.

Zhinong Wei received the B.E. degree in power system and its automation from Hefei University of Technology, Hefei, China, in 1984, the M.Sc. and Ph.D. degrees in electrical engineering from Southeast University, Nanjing, China, and Hohai University, Nanjing, China, in 1987 and 2004, respectively. He is currently working as a Professor with the College of Energy and Electrical Engineering, Hohai University. His research interests include integrated energy systems, power system state estimation, smart distribution systems, and integration of distributed generation into power systems.